

Investigation of the (n, 2n) reaction cross sections of some neighbouring nuclei with and without deformation

E Tel¹, A Aydin^{2*}, M Übeyli³ and İ Demirkol¹

¹ Gazi University, Faculty of Arts and Science, 06500 Ankara, Turkey

² Kirikkale University, Faculty of Arts and Science, 71400 Kirikkale, Turkey

³ Gazi University, Faculty of Technical Education, 06500 Ankara, Turkey

E-mail: eyuptel@gazi.edu.tr

Received 25 February 2002, accepted 28 July 2004

Abstract : The (n, 2n) reaction cross section calculations for some neighbouring target nuclei either with deformation or without deformation have been made for an incident energy range of 8 - 24 MeV. In these calculations, the geometry dependent hybrid model and the exciton model consisting of the effects of pre-equilibrium emissions have been used. The exciton model has also been used to investigate the pre-equilibrium direct effects. Furthermore, the experimentally measured cross sections taken from literature have been calculated using other empirical and the semi-empirical formulae for the incoming energies which satisfy the condition $U_R = E_n + Q_{n,2n} = 6 \pm 1$ MeV. The theoretical and experimental results for some neighbour target nuclei with or without deformation have been compared. The obtained results have been discussed with the available experimental data, and found to be good in agreement.

Keywords (n,2n) cross section, deformation of nuclei, exciton model

PACS Nos. 24.10.-i, 25.40.-h

1. Introduction

The knowledge of (n, 2n) cross section is very important and necessary in the reactor technology since a significant portion of the fission neutron spectrum lies above the threshold of (n,2n) reaction for the most of the reactor materials. Fusion serves an inexhaustible energy for humankind. Although there have been significant research and development studies on the inertial and magnetic fusion reactor technology, there is still a long way to go to penetrate commercial fusion reactors to the energy market. Neutronic characterization and development of structural materials, neutron multiplier materials, tritium breeders are primarily important for these types of reactors. Therefore, (n,2n) reactions of the selected blanket materials can play a key role for multiplying neutrons in reactor environment. In order to improve neutron economy, beryllium, lead, bismuth, zirconium are considered and used as neutron multiplier materials in fusion reactor design. In addition, thorium is a fertile fuel and can be transmuted to a very valuable fissile fuel ^{233}U to use in conventional nuclear fission reactors so that it is required to

determine the precise cross sections of thorium either experimentally or theoretically.

For many years, it has been customary to divide nuclear reactions into two extreme categories. First there are very fast, direct reactions which on a time scale comparable to the time ($\cong 10^{-22}$ s) necessary for the projectile to traverse a nuclear diameter, involve simple nuclear excitations, and are non-statistical in nature. At the other extreme, we have the compound nucleus reactions which occur on a very much longer time scale ($\cong 10^{-16}$ to 10^{-18} s) where emissions can be treated by the nuclear statistical model. This process can be described adequately by the Weisskopf-Ewing [1] (in 1940) and Hauser-Feshbach [2] (in 1952) compound nucleus theories. Compound nucleus wavefunction is very complicated, involving a large number of particle-hole excitations to which statistical considerations are applicable. This spectra of the emitted particles are approximately Maxwellian, and angular distributions of emitted particles are symmetric about 90 degrees.

During the nineteen-fifties and sixties, evidence accumulated suggesting that in some nuclear reactions, it is not possible to

* Corresponding Author

understand all emission processes in terms of compound nucleus and direct processes. Deviations from a Maxwellian shape for the emission spectra were observed for intermediate to high emission energies, with the theory under predicting data. The first developments were made to understand these observations by Griffin [3] (in 1966), who proposed the pre-equilibrium 'exciton model'. Pre-equilibrium processes are important mechanisms in nuclear reactions induced by light projectiles with incident energies above about 10 MeV. After Griffin introduced the exciton model, a series of semi-classical models [4-6] of varying complexities have been developed for calculating and evaluating particle emissions in the continuum. It was also shown that with some freedom in the choice of parameters, these models could give reasonable fit to the observed energy and angular distributions of the emitted particles. More recently, researchers have formulated several quantum-mechanical reaction theories [7] that are based on multi-step concepts and in which statistical evaporation at lower energies is connected to direct reactions at higher energies.

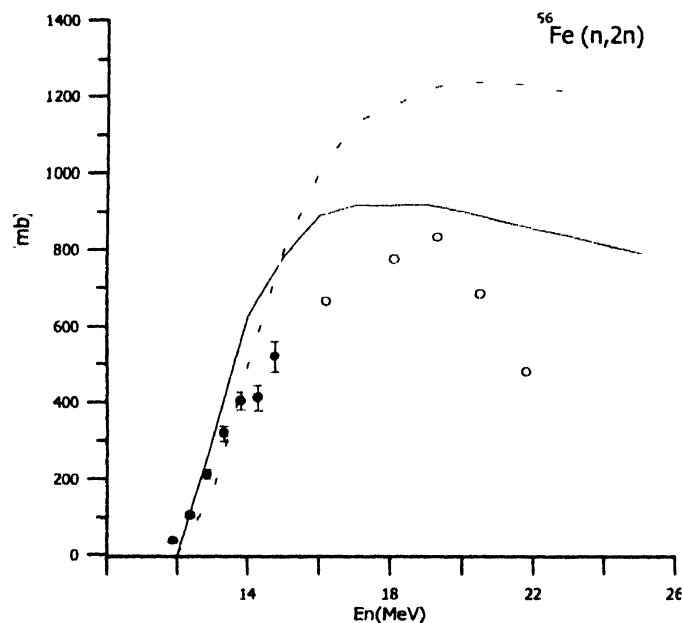


Figure 1. The calculated and experimental (n,2n) cross section for $^{56}\text{Fe}(n,2n)$. — exciton model plus evaporation, - - - GDH model plus evaporation; o experimental data were taken from Ref.[33]; • experimental data were taken from Ref.[34].

The character of the nuclear deformation can be seen in the mass regions $150 < A < 190$ and $A > 220$. The knowledge of the (n,2n) cross sections belonging to deformed and/or undeformed region should be useful for studying the accuracy of the statistical model. In the previous study, comparison of theoretical and experimental (n,2n) cross sections for deformed nucleus in the mass region of $150 < A < 190$ was made in details[8]. In this study, by using equilibrium and pre-equilibrium reaction mechanisms, the (n,2n) cross section values for some neighbour deformed and undeformed target nuclei between 8 and 24 MeV

incident energy for the isotopes, ^{56}Fe , ^{59}Co , ^{91}Zr , ^{93}Nb , ^{181}Ta , ^{182}W , ^{207}Pb , ^{209}Bi , and ^{232}Th have been calculated and compared with the experimental results.

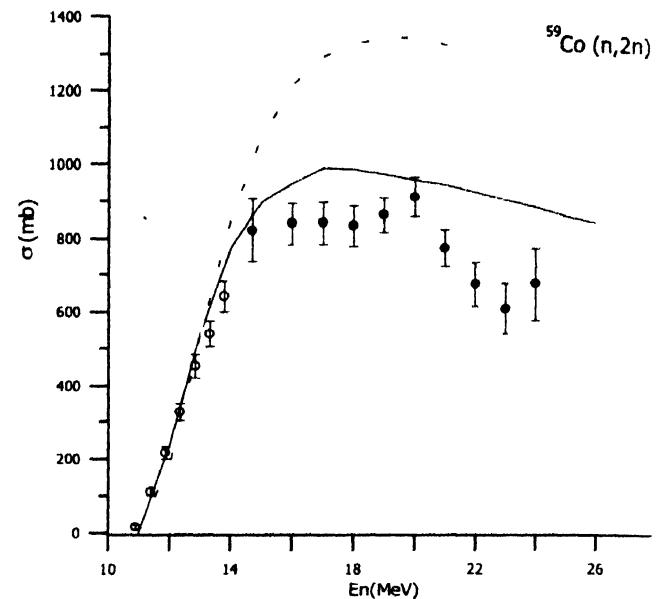


Figure 2. The calculated and experimental (n, 2n) cross section for $^{59}\text{Co}(n,2n)$. The solid curve is exciton model plus evaporation, - - - GDH model plus evaporation. o experimental data were taken from Ref.[34]; • experimental data were taken from Ref.[35]

2. Exciton model

Equilibrium emission is calculated according to the Weisskopf-Ewing (WE) model [1] by neglecting angular momentum. In the

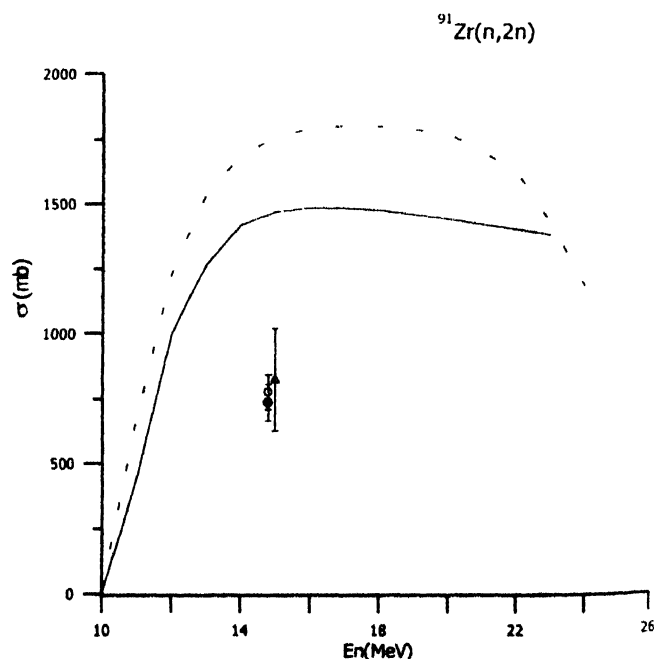


Figure 3. The calculated and experimental (n,2n) cross section for $^{91}\text{Zr}(n,2n)$. — exciton model plus evaporation; - - - GDH model plus evaporation; o experimental data were taken from Ref.[36], • experimental data were taken from Ref.[37]; Δ experimental data were taken from Ref.[38].

evaporation, the basic parameters are binding energies, inverse reaction cross section, the pairing and the level-density parameters.

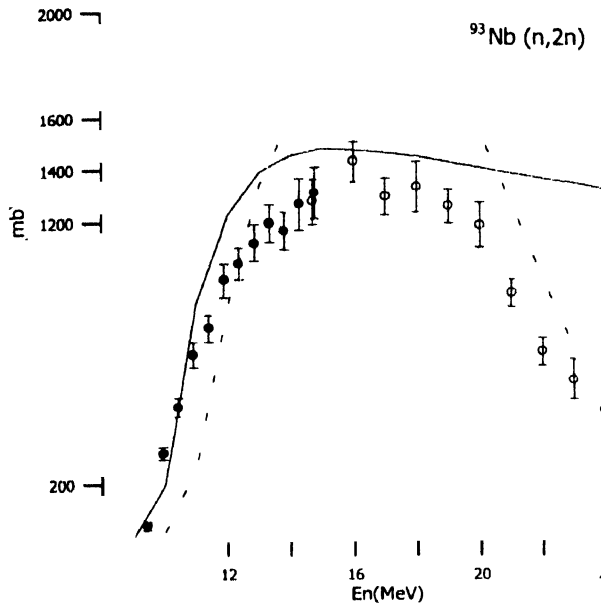


Figure 4. The calculated and experimental $(n, 2n)$ cross section for $^{93}\text{Nb}(n, 2n)$ — exciton model plus evaporation, - - - GDH model plus evaporation; o experimental data were taken from Ref [35], • experimental data were taken from Ref [34]

The exciton model assumes that after the initial interaction between the incident particle and the target nucleus, the excited system can pass through a series of stages of increasing complexity before equilibrium is reached, and emission may occur from these stages, giving the pre-equilibrium particles. The different stages of complexity are classified according to the

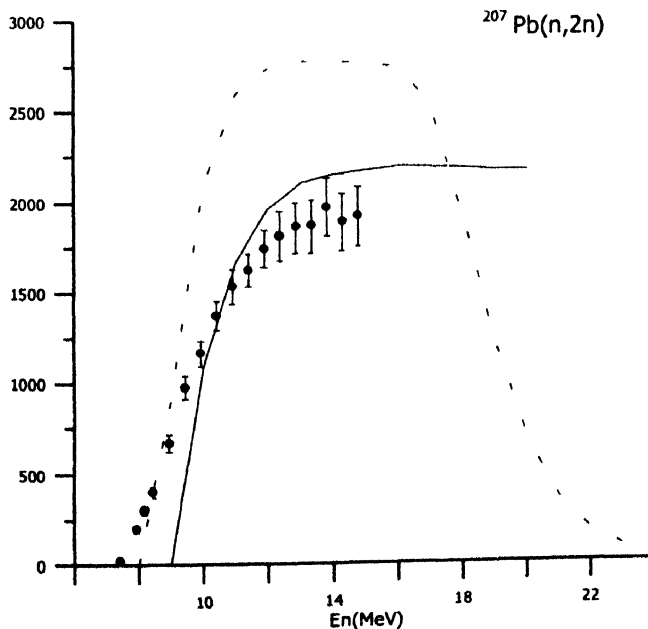


Figure 5. The calculated and experimental $(n, 2n)$ cross section for $^{207}\text{Pb}(n, 2n)$. — exciton model plus evaporation; - - - GDH model plus evaporation; • experimental data were taken from Ref.[34].

number of particles and holes excited, and the exciton model calculations involve solving a series of master equations that describe the equilibration of an excited system through a series of two-body collisions producing more complex configurations of particle-hole pairs. The master equation [9] over time is

$$\frac{dP}{dt}(n, t) = \lambda^+(n-2) P(n-2, t) + \lambda^-(n+2) P(n+2, t) - [\lambda^+(n) + \lambda^-(n) + W_t(n)] P(n, t), \quad (1)$$

where $P(n, t)$ is probability that the excited nuclear system exists in the exciton state n ($n = p + h$, the number of particles plus holes excited) at time t ; $\lambda^+(n)$ and $\lambda^-(n)$ are the internal transition rates for $n \rightarrow n+2$ and $n \rightarrow n-2$, respectively; $W_t(n)$ is total particle emission rate from stage n summed over all outgoing particles and energies. Expressions formally identical to the conventional Weisskopf's ones for the evaporation from the compound nucleus are thus obtained, with

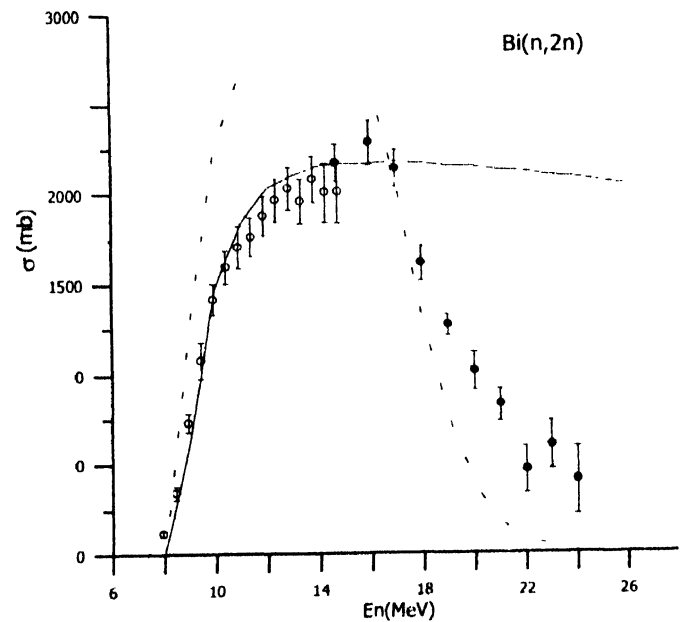


Figure 6. The calculated and experimental $(n, 2n)$ cross section for $^{209}\text{Bi}(n, 2n)$ — exciton model plus evaporation, - - - GDH model plus evaporation; o experimental data were taken from Ref [34], • experimental data were taken from Ref [35].

the only difference deriving from the introduction of the densities of particle (p) and hole (h) states. In order to solve the system of algebraic equations (1), the algorithm proposed by Akkermans *et al* [10] which gives an accurate result for any initial condition of the problem. The initial condition for solution of these equations is

$$P(p, h, 0) = \delta(p, p_0) \delta(h, h_0), \quad (2)$$

where the initial particle number is $p_0 = 2$ and initial hole number is $h_0 = 1$ for nucleon-induced reactions.

It is well known that during nucleon scattering in vibrational

nuclei, there occur processes of direct excitation of low excitation energy levels of collective type. At the latest specialists' meetings on nuclear data calculation, it was pointed out that a correct description of the high-energy emission spectrum in neutron-induced reactions could be obtained only if direct processes were taken into account. The experimental evidence

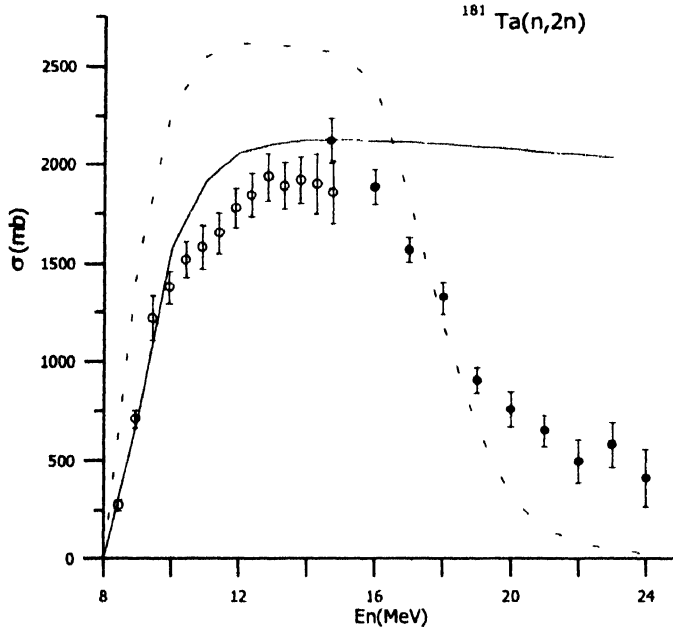


Figure 7. The calculated and experimental (n,2n) cross section for $^{181}\text{Ta}(n,2n)$. — exciton model plus evaporation; - - - GDH model plus evaporation; o experimental data were taken from Ref.[28], • experimental data were taken from Ref [31]

in support of this type of mechanism has been confirmed by the latest experiment with the (n, n') reactions with a very good resolution [11,12]. In the experimental spectra, we can clearly see a structure of peaks which corresponds to the excitations of the direct type. A parametrization was adopted in Ref.[13] to describe this phenomenon. In accordance with this parametrization, the differential cross-section of neutron emission by the direct interaction in the (n, n') reaction can be written as

$$\frac{d\sigma_{ab}^{dir}}{d\varepsilon_b}(\varepsilon_b) = \left[\frac{2\mu}{\hbar^2} \right] \frac{V}{(k_a R)^2} \frac{k_b}{k_a} P_a(\varepsilon_a) P_b(\varepsilon_b) \times V_R^2 \sum_{\lambda=2}^3 \frac{\beta_\lambda^2}{(2\lambda+1)} \delta(U - \omega_\lambda) \quad (3)$$

where V , R , V_R , are the volume of the nuclei, the radius of nuclei and the potential well depth taken to be 48 MeV, respectively. $P_a(\varepsilon_a) = 4k_a K_a / (k_a + K_a)$ is the coefficient of the penetrability, k_a and K_a being projectile wave numbers inside and outside the nucleus. β_λ and ω_λ are deformation and energy parameters which correspond to the target nucleus levels of the collective type. Only the octupolar and quadrupolar oscillations are considered. The ω_2, β_2 , values for even nuclei

were taken from Ref.[14]. In the case of odd nuclei, on the assumption of a weak bond, the values corresponding to the neighbouring even nucleus are used. The ω_3 value was taken from Ref.[15]. The octupolar deformation parameters were calculated from $\beta_3^2 = (2\lambda + 1)\omega_3$ [MeV]/1000. Capote *et al.*[13] have replaced the function $\delta(U - \omega_\lambda)$, which relates the excitation energy of the residual nucleus to the energy the collective state and to emission energy, by a Gaussian distribution whose semi-width is chosen by taking into account the experimental energy resolution. The parametrization used in eq. (3) assumes that the direct interaction is confined to the surface.

3. Hybrid and geometry dependent hybrid model

The hybrid model for pre-compound decay is given by Blann and Vonach [16] as

$$\frac{d\sigma_v(\varepsilon)}{d\varepsilon} = \sigma_R P_v(\varepsilon), \quad (4)$$

and

$$P_v(\varepsilon)d\varepsilon = \sum_{\substack{n=n_0 \\ \Delta n=+2}}^{\bar{n}} [{}_n\chi_v N_n(\varepsilon, U) / N_n(E)] g d\varepsilon \times \left[\lambda_r(\varepsilon) / (\lambda_r(\varepsilon) + \lambda_+(\varepsilon)) \right] D_n, \quad (5)$$

where σ_R is the reaction cross section, ${}_n\chi_v$ is the number of particle type v (proton or neutron) in n exciton hierarchy, represents number of particles of the n (neutron or proton) emitted into the unbound continuum with channel energy between ε and $\varepsilon + d\varepsilon$. The quantity in the first set of square

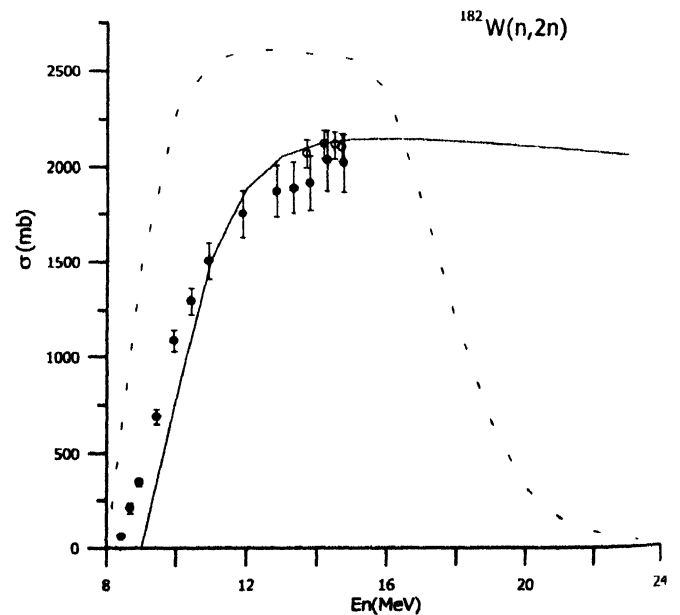


Figure 8. The calculated and experimental (n,2n) cross section for $^{182}\text{W}(n,2n)$. — exciton model plus evaporation; - - - GDH model plus evaporation; o experimental data were taken from Ref.[39]; • experimental data were taken from Ref.[28].

brackets of eq.(5) represents the number of particles to be found (per MeV) at a given energy ϵ for all scattering processes leading to an n exciton configuration. $\lambda_c(\epsilon)$ is emission rate of a particle into the continuum with channel energy ϵ and $\lambda_+(\epsilon)$ is the intranuclear transition rate of a particle. It has been demonstrated that the nucleon-nucleon scattering energy partition function $N_n(E)$ is identical to the exciton state density $\rho_n(E)$, and may be derived by the certain conditions on N-N (nucleon-nucleon) scattering cross sections [17]. The second set of square brackets in eq.(5) represents the fraction of the v type particles at the energy which should undergo emission into the continuum, rather than making an intranuclear transition. The D_n represents the average fraction of the initial population surviving to the exciton number being treated.

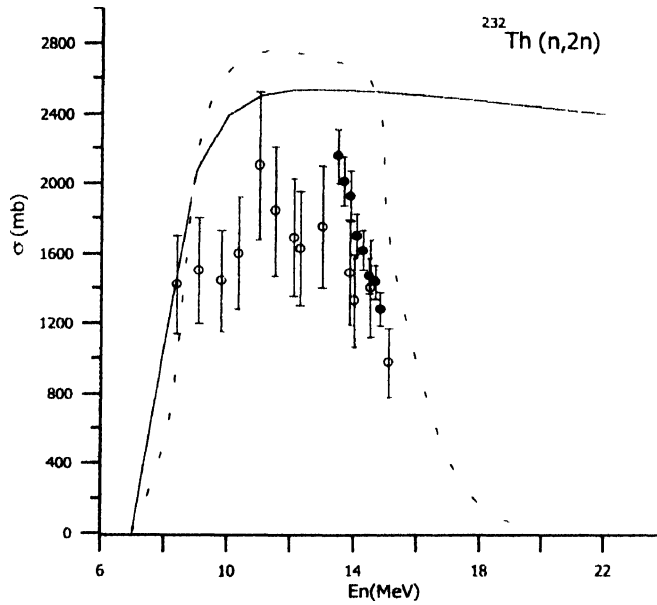


Figure 9. The calculated and experimental (n,2n) cross section for $^{232}\text{Th}(n,2n)$. — exciton model plus evaporation, - - - GDH model plus evaporation, o experimental data were taken from Ref.[40], • experimental data were taken from Ref [41].

The hybrid model was reformulated by Blann and Vonach [16], as the geometry dependent hybrid model (GDH) to crudely incorporate the effects of the diffuse nuclear surface sampled by the higher impact parameters. The differential emission spectrum is given in the GDH as

$$\frac{d\sigma_v(\epsilon)}{d\epsilon} = \pi \lambda^2 \sum_{l=0}^{\infty} (2l+1) T_l P_l(l, \epsilon), \quad (6)$$

where λ is the reduced de Broglie wavelength of the projectile and T_l represents transmission coefficient for l -th partial wave. Using the total pre-compound neutron emission spectrum $d\sigma_n(\epsilon)/d\epsilon$, the cross section which could be involved in the emission of two neutrons is calculated as

$$\sigma_{2n} = \int_{U=0}^{E-B_{2n}} \frac{a\sigma_n(\epsilon)}{d\epsilon} d\epsilon, \quad \text{where } B_{2n} \text{ represents the sum of the}$$

first and the second neutron binding energies.

4. Empirical and semi-empirical formulas for (n, 2n) reaction cross section

Q-value plays an important role on (n, 2n) cross sections at given incident neutron energy E_n . However, it is essential to look for the dependence of (n, 2n) cross sections on the asymmetry parameter at a given maximal residual excitation energy, $U_R = E_n + Q_{n,2n}$. The (n, 2n) reaction has been frequently investigated in the past. Until now, a large number of experimental data have been published on the (n, 2n) reaction cross sections induced by 14 to 15-MeV neutrons (see, for example, the Computer index of Neutron Data bibliographic catalogue). Most of the experimental data are taken at energies near 14-MeV neutron energy. There are several formulae describing the isotopic dependence of cross sections for different reactions at neutron energy of 14.5 MeV. The measured cross sections exhibit a large gradient for the lighter masses ($Z \leq 30$) with increasing asymmetry parameter and then become almost constant for medium and heavy mass nuclei (starting from $A \leq 100$) [18]. Recently as well as many years ago various attempts [19-23] were made to describe the compiled experimental values by relating the neutron-induced cross sections to the $s = (N - Z)/A$ asymmetry parameter.

Adam and Jeki [20] formulated as (in mb)

$$\sigma_{n,2n} = 2050 \left[1 - 0.061 (A^{1/3} + 1)^2 \exp(-8.6s) \right]. \quad (7)$$

Figure 10 illustrates the ratio of experimental to the calculated (n,2n) cross sections for the incident energies E_n at which

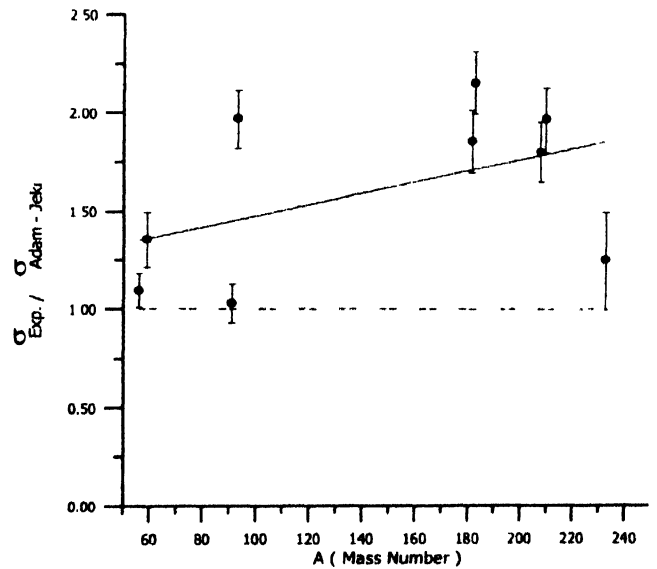


Figure 10. The ratios of experimental (n,2n) cross sections to the present compound-nucleus calculations versus the atomic mass number of the target nuclei, for $U_R = 6 \pm 1$ MeV — the linear function $y(A) = \sigma_{\text{exp}}/\sigma_{\text{calc}} = 0.00289294A + 1.18765$, obtained by least-squares fit to the data.

the condition $U_R = E_n + Q_{n,2n} = 6 \pm 1$, where U_R is the excitation energy of the residual nucleus. One can see from Figure 10 that the experimental values for the nuclides ($A < 100$) without deformation and Th ($A > 220$) with deformation are about 10-15 % higher than calculated (n,2n) cross sections by using the Adam-Jeki formula. However, for the nuclides ($150 < A < 190$) with deformation they reach a value of 50-60 % higher than theoretical calculated results with respect to the Adam-Jeki formula.

Bychkov *et al* [21] have formulated (n,2n) cross sections as

$$\sigma_{n,2n} = \begin{cases} 1000 + 7.5A(7.8s - 0.234) & \text{if } s \leq 0.13 \\ 1000 + 7.5A(0.65 + s) & \text{if } s > 0.13 \end{cases} \quad (8)$$

The ratio of experimental to the calculated (n,2n) cross sections is depicted in Figure 11. The experimental values for the nuclides ($A < 100$) without deformation and Th ($A > 220$) with deformation are about 30-40 % lower than calculated (n,2n) cross sections with respect to the formula of Bychkov *et al* [21]. Nevertheless, for the nuclides ($150 < A < 190$) with deformation they reach a value of 10-15 % lower than the results for formula of Bychkov *et al*.

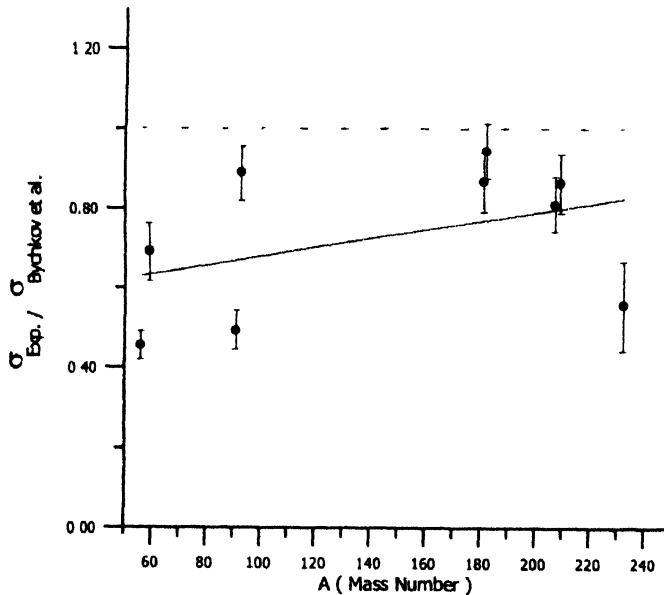


Figure 11. The ratios of experimental (n,2n) cross sections to the present compound-nucleus calculations versus the atomic mass number of the target nuclei, for $U_R = 6 \pm 1$ MeV. — the linear function $y(A) = \sigma_{\text{exp}}/\sigma_{\text{calc}} = -0.00110466A + 0.568337$, obtained by least-squares fit to the data

Konno *et al* [22] have suggested a phenomenological formula for 14.9 MeV neutrons (in mb) as follows :

$$\ln(\sigma_{n,2n}) = 7.434 [1 - 1.484 \exp(-27.37 s)] \quad (9)$$

Figure 12 shows the ratio of experimental to the calculated (n,2n) cross sections for the incident energies E_n for the

condition $U_R = E_n + Q_{n,2n} = 6 \pm 1$ MeV, where U_R is the excitation energy of the residual nucleus. The experimental values for the nuclides ($A < 100$) without deformation and the nuclides ($150 < A < 190$) with deformation are about 30-40 % and 10-15 % higher than the calculated (n,2n) cross sections according to the formula of Konno *et al*, respectively. However, for ^{232}Th they are 10-15 % lower than calculated results based on the formula of Konno *et al*.

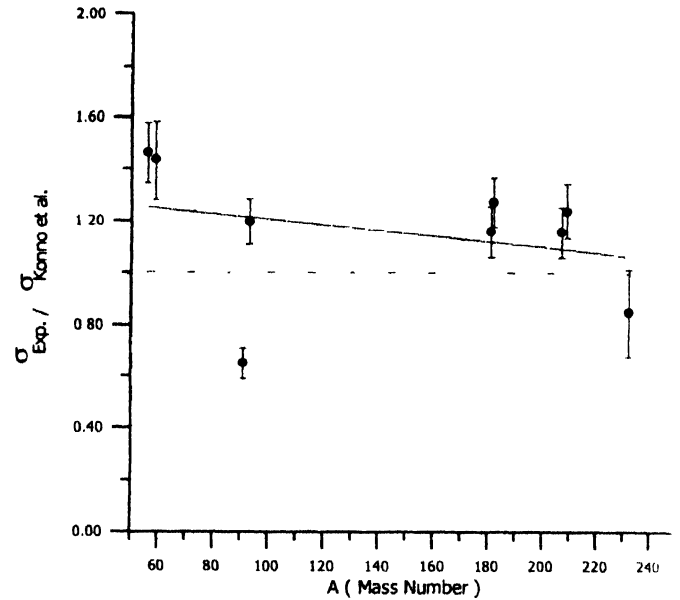


Figure 12. The ratios of experimental (n,2n) cross sections to the present compound-nucleus calculations versus the atomic mass number of the target nuclei, for $U_R = 6 \pm 1$ MeV. — the linear function $y(A) = \sigma_{\text{exp}}/\sigma_{\text{calc}} = -0.00109162A + 1.31654$, obtained by least-squares fit to the data.

The (n,2n) reaction cross sections were also studied by Pearlstein [23] using the following formula,

$$\sigma_{n,2n}(E) = \sigma_{ne} \frac{\sigma_{n,M}}{\sigma_{ne}} \frac{\sigma_{n,2n}(E_{inc})}{\sigma_{n,m}}, \quad (10)$$

where E_{inc} is the incident neutron energy and σ_{ne} nonelastic cross section. The sum of the (n, n'), ($n, 2n$), ($n, 3n$), etc, cross sections belonging to this class is given the symbol $\sigma_{n,M}$.

The ratio $\sigma_{n,M}/\sigma_{n,e}$ is empirically determined by Barr *et al* [24]

$$\sigma_{n,M}/\sigma_{n,e} = 1 - 1.764 \exp[-18.14 s]. \quad (11)$$

The ratio of experimental to the calculated (n,2n) cross sections by taking the Pearlstein formula as reference is shown in Figure 13. Except for ^{232}Th , one can see generally from this figure that by going from the nuclides without deformation to the nuclides with deformation the agreement between the experimental and theoretical values increases. The parameters used in the calculations are given in the Table 1. Reaction Q-

Table 1. Experimental cross sections for (n,2n) reactions at $U_R = 6 \pm 1$ MeV

Nuclear reaction	$Q_{n,2n}$ value (MeV)	Threshold energy (MeV)	$(N-Z)_R$	E_n (MeV)	$\sigma_{n,2n}$ (mb)	Ref
$^{56}_{25}\text{Fe}(n,2n)^{55}_{25}\text{Fe}$	-11 19732	11 40675	3	14.76 ± 0.06	519 ± 41	[34]
$^{59}_{27}\text{Co}(n,2n)^{58}_{27}\text{Co}$	-10 4535	10.6387	4	14.70 ± 0.06	820 ± 85	[35]
$^{91}_{41}\text{Zr}(n,2n)^{90}_{40}\text{Zr}$	-7 1945	7.2762	10	14.80 ± 0.00	734 ± 70	[37]
$^{93}_{41}\text{Nb}(n,2n)^{92}_{41}\text{Nb}$	-8 8311	8 9291	10	14.76 ± 0.06	1313 ± 99	[34]
$^{181}_{73}\text{Ta}(n,2n)^{180}_{73}\text{Ta}$	-7 5770	7 6197	34	14.76 ± 0.06	1856 ± 159	[28]
$^{182}_{74}\text{W}(n,2n)^{181}_{74}\text{W}$	-8 064	8 110	33	14.76 ± 0.06	2017 ± 150	[28]
$^{207}_{82}\text{Pb}(n,2n)^{206}_{82}\text{Pb}$	-6 73779	6 77095	42	14.28 ± 0.07	1888 ± 160	[34]
$^{209}_{83}\text{Bi}(n,2n)^{208}_{83}\text{Bi}$	-7.4598	7 4961	42	14.76 ± 0.65	2018 ± 170	[34]
$^{232}_{90}\text{Th}(n,2n)^{231}_{90}\text{Th}$	-6 4381	6 4664	51	14.50 ± 0.00	1400 ± 280	[40]

values and threshold energy were taken from Audi and Wapstra [25].

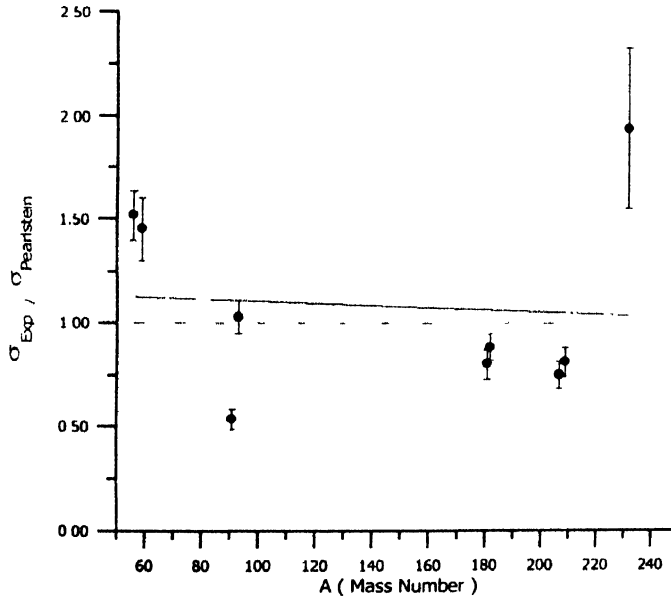


Figure 13. The ratios of experimental (n,2n) cross sections to the present compound-nucleus calculations versus the atomic mass number of the target nuclei, for $U_R = 6 \pm 1$ MeV. — the linear function $y(A) = \sigma_{\text{exp}}/\sigma_{\text{cnk}} = -0.000477397A + 1.14897$, obtained by least-squares fit to the data.

5. Results and discussion

In this study, (n, 2n) reaction cross sections for the isotopes ^{56}Fe , ^{59}Co , ^{91}Zr , ^{93}Nb , ^{181}Ta , ^{182}W , ^{207}Pb , ^{209}Bi and ^{232}Th have been calculated using equilibrium and pre-equilibrium reaction mechanisms. The equilibrium calculations have been made by using Weisskopf-Ewing (WE) model, while exciton model and geometry-dependent hybrid model were used for pre-equilibrium

calculations. The calculations have been made in the framework of the GDH model using ALICE/LIVERMORE-82 computer code [26]. Theoretical calculations have also been made in the framework of the exciton model using PCROSS computer code [13]. The calculated excitation functions have been obtained on the basis of the exciton model and geometry-dependent hybrid model. In Figures 1 to 9, the theoretically calculated (n, 2n) cross-section values have been compared with the experimental values, which were taken from Ref. [28,31,33-41].

PCROSS program code, in calculations of the exciton model, uses the initial exciton number as $n_0 = 1$, thus taking into account the direct gamma emission. Equilibrium exciton number is taken equal to $\sqrt{1.4 gE}$, as was suggested in Ref. [27], after Pauli correction is modified. Single particle level density parameter g was equal to $A/13$ in the exciton model calculation, where A is the mass number. Level density expression given by Dilg *et al* [28] was used in the evaporation model calculation. Particle-hole state density expression reported by Williams [27] was used in the pre-equilibrium model calculation. The reaction cross-sections and the inverse cross sections were obtained using the optical potential parameters by Wilmore and Hodgson [29], Bechetti and Greenless [30], Huizenga and Igo [31] for neutrons, protons and alpha particles, respectively.

In the calculations of GDH model, ALICE/LIVERMORE-82 code uses the initial exciton number as $n_0 = 3$. This model requires the initial neutron (n) and proton (p) exciton numbers. In the calculations for neutron induced reactions, these exciton numbers are given by Blann and Vonach [16] as, ${}_3X_n = \frac{2(3Z+2N)}{(3Z+2N+3Z)}$ and ${}_3X_p = 2 - {}_3X_n$. N and Z are the neutron and proton numbers of the target nuclei, respectively. The standard pairing shift (zero for odd-even nuclei, delta for

odd-odd nuclei) proposed by Blann and Bisplinghoff [26] was employed as the pairing correction for GDH model calculation. In the GDH model, the level density expression using the formula with mass shell corrections was used for ^{56}Fe , ^{59}Co , ^{91}Zr , ^{93}Nb , ^{207}Pb , ^{209}Bi , and ^{232}Th . The Fermi-gas level density expression was used for ^{181}Ta and ^{182}W . The geometry dependence influences are manifested in two distinct manners in the formulation of the GDH model. The more obvious is the longer mean free path predicted for nucleons in the diffuse surface region. The second effect is less physically secure, yet seems to be important in reproducing experimental spectral shapes. The nuclear density distribution used in the GDH model is a Fermi density distribution function, $\rho(R_l) = \rho_s [\exp(R_l - C)/0.55 \text{ fm} + 1]^{-1}$, where ρ_s is the density at the center of nucleus, and $C = 1.07 A^{1/3} \text{ fm}$ taken from electron scattering results [32]. The radius for the l -th entrance channel partial was defined by $R_l = \lambda_l(1 + 1/2)$. In GDH model, the Fermi energies and nuclear densities are defined to impact parameter R_l .

In this study, the exciton model for the incident neutron energies about 14-15 MeV is very successful for all the neighbouring nuclei with and without deformation nuclei (except ^{91}Zr). The GDH model calculations for the same energies are higher than the experimental values for neighbouring nuclei with and without deformation nuclei. Moreover, the prediction of GDH model is about 10-15% higher than that of exciton model in the region of $U_R = E_n + Q_{n,2n} = 6 \pm 1 \text{ MeV}$. However, GDH prediction of model is more successful than exciton model for the incident neutron energy above 15 MeV. Both models were used together with the Weisskopf-Ewing (WE) model for equilibrium calculation. The exciton model (PCROSS) code uses a master equation and treat equilibrium and pre-equilibrium in a 'unified' way. The GDH model involves incoming orbital angular momentum l in order to account for the effects of the nuclear-density distribution. This leads to increased emission from the surface region of the nucleus, and thus to increase emission of high-energetic particles.

Besides, the $(n,2n)$ cross sections have been calculated using other empirical and semi-empirical formulae for the incoming energies which satisfy the condition $U_R = E_n + Q_{n,2n} = 6 \pm 1 \text{ MeV}$. All empirical and semi-empirical formulae used in this study are very successful for calculating $(n,2n)$ cross section of ^{93}Nb . However, for ^{91}Zr , the difference between the theoretical and experimental results is quite large.

Especially in the region of $U_R = 6 \pm 1 \text{ MeV}$, there is a good agreement between the experimental data and the calculated values using Pearlstein formula, which is a semi-empirical formula while other formulae considered in this study, are empirical. Consequently, evolution of semi-empirical formulae is very

important to understand and develop nuclear models and nuclear reaction theories.

Acknowledgment

This work has been supported by the State Planning Organization of Turkey, Project # DPT-2003K 120470-08.

References

- [1] V F Weisskopf and D H Ewing *Phys. Rev.* **57** 472 (1940)
- [2] W Hauser and H Feshbach *Phys. Rev.* **87** 366 (1952)
- [3] J J Griffin *Phys. Rev. Lett.* **17** 478 (1966)
- [4] M Blann *Annu. Rev. Nucl. Sci.* **25** 123 (1975)
- [5] E Betak *Comp. Phys. Commun.* **9** 92 (1975) Institute of Physics, Slovak Academy of Science, Dubravska cesta, 899 50 Czechoslovakia (PREEQ Program Code)
- [6] H. Gruppelaar, P Nagel, P E Hodgson and LaRivasta *Del Nuovo Cim* **9** 1 (1986)
- [7] H Feshbach, A Kerman and S Koonin *Annu. Phys.* (NY), **125** 429 (1980)
- [8] E Tel, S Okuducu, A Aydin, B Sarer and G Tanir *Acta Phys. Slov.* **54** 191 (2004)
- [9] C K Cline *Nucl. Phys.* **A193** 417 (1972)
- [10] J M Akkermans, H Gruppelaar and G Reffo *Phys. Rev.* **C22** 77 (1980)
- [11] M Baba, M Ishikawa, N Yabuta, T Kikuchi, H Wakabayashi and M Mirakawa *Int Conf on Nucl. Data for Science and Technology* (May-June 1988, Mito, Japan)
- [12] A Pavlik and H Vonach *Report IRK* (Vienna) (1988)
- [13] R Capote, V Osorio, R Lopez, E Herrera and M Pires *Final Report on Research* contract 5472/RB, INDC(CUB)-004 (Higher Institute of Nuclear Science and Technology, Cuba) Translated by the IAEA on the March 1991. (PCROSS program code)
- [14] S Raman, C H Malarkey, W T Milner, C W Nestor, J R and P H Stelson *Atomic Data & Nuclear Data Tables* **36** 1 (1987)
- [15] C M Lederer, V S Shirley *Table of Isotope* (1978)
- [16] M Blann and H K Vonach *Phys. Rev.* **C28** 1475 (1983)
- [17] M Blann, A Mignerey and W Scobel *Nukleonika* **21** 335 (1976)
- [18] E Betak, T Kempisty and S Raman *Nucl. Sci. Eng.* **132** 295 (1999)
- [19] E Tel, B Sarer, S Okuducu, A Aydin and G Tanir *J. Phys.* **G29** 2169 (2003)
- [20] A Adam and L Jeki *Acta Phys. Acad. Sci. Hung.* **26** 335 (1969)
- [21] V M Bychkov, V N Manokhin, A B Pashchenko and V I Plyaskin *Handbook of Cross Sections for Neutron Induced Threshold Reactions* (Energoizdat, Moskova) (1982), (in Russian)
- [22] C Konno, Y Ikeda, K Oishi, K Kawade, H Yamamoto and H Maekawa *JAERI-1329, Japan Atomic Energy Research Inst* (1993)
- [23] S Pearlstein *Analysis of $(n, 2n)$ Cross section for Nuclei of Mass, $A \geq 30$* , BNL-897, (Brookhaven National Laboratory) (1964)
- [24] D W Barr, C I Browne and J S Gilmore *Phys. Rev.* **123** 859 (1961)
- [25] G Audi and A H Wapstra *Nucl. Phys.* **A595** 409 (1995)
- [26] M Blann and J Bisplinghoff *"CODE ALICE/LIVERMORE 8.2"* UCID-19614 (1982)
- [27] F C Williams *Nucl. Phys.* **A166** 231 (1971)
- [28] W Dilg, W Schantl, H Vonach and M Uhl *Nucl. Phys.* **A217** 269 (1973)

- [29] D Wilmore and P E Hodgson *Nucl. Phys.* **55** 673 (1964)
- [30] F D Becchetti and G W Greenlees *Phys. Rev.* **182** 1190 (1969)
- [31] J R Huizenga and G Igo *Nucl. Phys.* **29** 462 (1962)
- [32] R Hofstadter *Annu. Rev. Nucl. Sci.* **7** 295 (1957)
- [33] V Corcalciuc, B Holmqvist, A Marcinkowski and G A Prokopets *Nucl. Phys.* **A307** 445 (1978) and P, KDK- 23, 35,7804) (P, KDK-12,8,7604),(P,S-501,21,7509)-A Study of the Neutron Induced Reactions for F-19, Fe-56,Co-59 in the Energy Interval 16 to 22 MeV-
- [34] J Frehaut, A Bertin, R Bois and J Jary *Status of (n,2n) Cross section Measurements at Bruyeres -Le-Chatel*, Supersedes all former publications (C, 75KIEV, 7506), Full paper of contribution to symposium on neutron Cross sections from 10-50 MeV, (Upton L I U S A), May, 12-14, (1980)
- [35] L R Veaser, E D Arthur and P G Young *Phys. Rev. C* **16** (1977) 1792 *Cross sections for (n,2n) and (n,3n) Reaction above 14 MeV* (C,76LOWELL,2,1351(PH2/F13),197607)
- [36] S Ameniya, V N Bhoraskar, K Katoh and T Katoh *J. Nucl. Sci. Technol.* **18** 323 (1981)
- [37] T Sothias *Dissertation Abstracts B (Sciences)* **38** 280 (1978)
- [38] G Peto, P Bornemisza Pausperli and J Karolyi (J.AHP,25,91, 6810) *Expt. Details and Data Applicability of the Statistical Model for Explaining the Ratio of the Inelastic/(n,2n) Cross sections*
- [39] Kong Xiangzhong, Hu Shangbin and Yang Ingkang (J,CNDP, 17,9,199706) *Cross sections of 14 MeV neutron induced reactions on Wolfram isotopes*
- [40] H A Tewes, A A Caretto, A E Miller and D R Nethaway (R,UCRL-6028- T,6006), *Excitation Functions of Neutron induced Reactions*
- [41] A A Filatenkov, S V Chuvaev, V N Aksenov, V A Yakovlev, A V Malyshev, S K Vasil'ev, M Avrigeanu, V Avrigeanu, D L Smith, Y Ikeda, A Wallner, W Kutschera, A Priller, P Steier, H Vonach, G Mertens and W Rochow (R,R1-252,199905) , R,INDC(CCP) 402,199701), (J,YK,1996,(2),8,199612), (C,97TRIEST,1,595, 199705) 59-Co, 58-Ni, (C,97TRIEST,2,1248,199705) Al-27(n,2n), *Systematic Measurement of Activation Cross Sections at Neutron Energies from 13.4 to 14.9 MeV*